WMO/IOC/UNEP/ICSU
GLOBAL CLIMATE OBSERVING SYSTEM (GCOS)

Doc. 5.3
(24.II.2012)

4th GRUAN Implementation-Coordination Meeting (ICM-4)
Tokyo, Japan
5 March – 9 March 2012

Session 5

Site Report: Tateno, Japan

(Submitted by Hironobu Yokota, Nobuhiko Kizu, Yoshiyuki Noto, Ryo Yoshida and Yoshiaki Sato, Japan Meteorological Agency)

Summary and Purpose of Document

This document outlines the development and status of the Tateno site, and also reports on related activities carried out by the Japan Meteorological Agency (JMA) in the areas of GPS-PWV, NWP and its upper-air observational network.

PART 1 TATENO SITE STATUS AND RECENT CONTRIBUTIONS TO GRUAN

1.1 Overview and History of the Tateno Site

Tateno (47646) is the name of a Japan Meteorological Agency (JMA) aerological observatory located in Tsukuba City (36°03'N, 140°08'E, 31 m AMSL) approximately 52 km northeast of Tokyo (Fig. 1.1).

The observatory was established in April 1920 by the forerunner of JMA with Wasaburo Ooishi as its first director (Table 1.1). After the facility was opened, upper-air wind observation was conducted for the first time using a small pilot balloon in April 1921, and lower-atmosphere observation was implemented using a kite and a tethered balloon in line with technologies adopted in Germany (the kite method was discontinued in February 1946). A radiosonde capable of sending signals via electric waves was subsequently developed and used for observation from 1946. Routine observation began in 1952, and the observatory's organization as it stands today was formed to coincide with its participation in the International Geophysical Year (IGY) in 1957.

When the facility was founded, Ooishi and others discovered a strong westerly wind (known today as the jet stream) in the upper air over Japan via pilot balloon observation. Although they reported their finding to the world in Esperanto*, little attention was paid to it at the time. When the jet stream was noticed again by American researchers around 20 years later, the achievements of the jet stream discovery by Oishi and others gained full recognition.

Tateno conducts surface observation and lower-atmosphere (up to 1.5 km) observation by using a tethered balloon, upper-atmosphere (up to about 30 km) observation by using radiosondes, observation of ozone vertical distribution using ozonesondes, observation of total ozone using a Dobson ozone spectrophotometer, ultraviolet observation using a Brewer spectrophotometer, and radiation observation. In its role as a technical center for aerological observation in Japan and Asia, the observatory has responsiblities to develop and improve methods and instrumentation for upper-air observation and to provid training for meteorological experts of JMA.

Tateno adjoins JMA's Meteorological Instruments Center, that guarantees the traceability to SI standard about weather instruments accuracy.

Table 1.1 History of Tateno

Aug. 1920	The aerological observatory was founded.
Nov. 1920	Surface observation was started.
Apr. 1921	Upper-air wind observation was started. A small hydrogen balloon was launched and tracked using optical theodolites.
Dec. 1922	Lower-atmosphere observation was started using a kite and a tethered balloon. (Kite usage was discontinued in February 1946.)
Dec. 1924	Ooishi discovered strong westerly winds* (the jet stream)**.
Aug. 1925	Sounding-balloon observation was started. A large balloon equipped with an aerometeorograph was launched and recovered when it came down to allow reading of atmospheric pressure, temperature and humidity recordings.
Sep. 1944	Radiosonde observation was started.
Nov. 1948	Rawin observation (wind sounding) was started (discontinued in March 2004).
Jul. 1955	Atmospheric ozone observation using a Dobson spectrophotometer was started.
Jul. 1957	Observation of solar and terrestrial radiation was started.
Sep. 1959	Radioactivity-sonde observation was started (discontinued in March 2006).
Mar. 1968	Ozonesonde observation was started.
Mar. 1986	An automatic data processing system was introduced for aerological observation.

Aug. 1988	Surface ozone observation was started.
Jan. 1990	Solar spectral ultraviolet radiation observation using a Brewer spectrophotometer was started.
Feb. 1992	New ground facilities for the JMA-91-type aerological observation system were introduced to support observation.
Oct. 1992	A new radiosonde (RS2-91 type) was introduced for aerological observation.
Feb. 1993	The WMO International Radiosonde Comparison Phase IV meeting was held at the observatory.
Jan. 1994	The automatic Dobson ozone spectrophotometer was developed.
Mar.1995	The observatory was registered as a site in the GCOS Upper-air Network (GUAN).
Feb. 1996	The International Workshops on Ozone Observation in Asia and the Pacific Region (IWOAP) event was held at the observatory.
Aug. 1996	The Second International Workshops on Ozone Observation in Asia and the Pacific Region (IWOAP-II) event was held at the observatory.
Jun. 1997	BSRN (Baseline Surface Radiation Network) reporting to World Radiation Center was started.
Jul. 1999	High-altitude observation was started for the collection of upper-air data at pressures of up to 5 hPa.
Mar. 2003	The WMO/GAW Regional Intercomparison of Dobson Spectrophotometers for Asia meeting was held at the observatory.
Mar. 2006	The Dobson Regional Intercomparison for Asia in Tsukuba (DIC-T2006) event was held at the observatory.
Sep. 2009	The observatory was registered as a site in the GCOS Reference Upper-air Network (GRUAN).
Nov. 2009	Measurement of total column water vapor using a ground-based GPS receiver was started.
Dec. 2009	Observation of wind profiles using Doppler lidar was started. The RS92-SGPJ-type GPS sonde was introduced to support aerological observation, and the ECC ozonesonde was introduced for ozonesonde observation.
May 2011	New ground facilities of the JMA-10-type aerological observation system were introduced to support observation.

* Ooishi, W., 1926: Raporto de la Aerologia Observatorio de Tateno (in Esperanto). Aerological Observatory Rep. 1, Central Meteorological Observatory, Japan, pp. 213.
** Lewis, J. M., 2003: Ooishi's observation: Viewed in the context of jet stream discovery. *Bull. Amer. Meteor. Soc.*, **84**, 357 – 369.

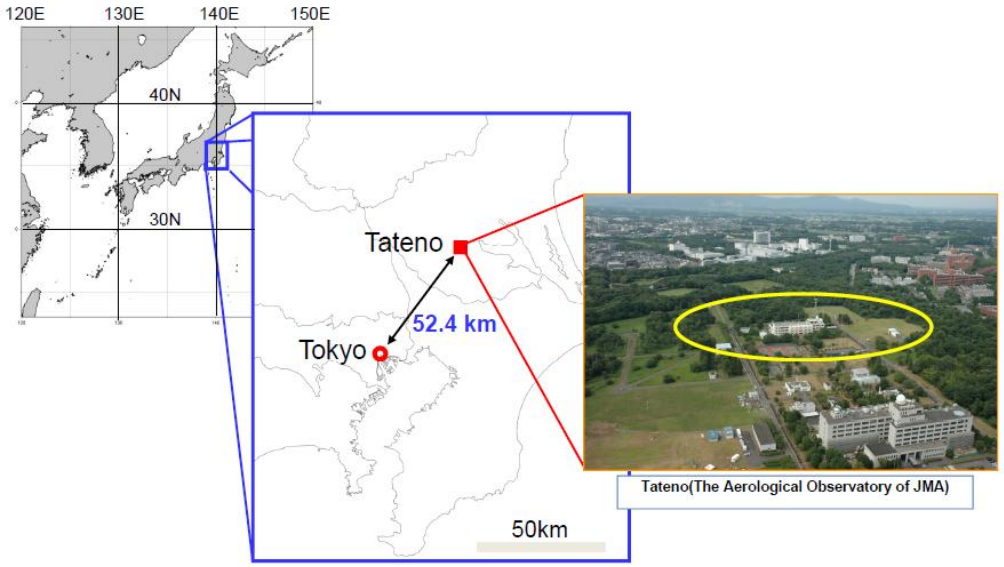

Figure 1.1 Location of Tateno (36°03'N, 140°08'E, 31 m AMSL)

1.2 Activities of Tateno site

1.2.1 Surface Observation

Surface observation has been carried out using new JMA-10-type surface meteorological observation equipment since May 2011. The parameters and equipment/methods of observation are listed in Table 1.2.

Table 1.2 Parameters and equipment/methods of surface observation at Tateno

Parameter	Equipment/method
Atmospheric pressure	Electric capacitive barometer
Air temperature	Platinum resistance thermometer*
Humidity	Electric capacitive hygrometer
Wind direction/speed	Wind vane/propeller anemometer*
Precipitation	Tipping-bucket rain gauge*
Snow	Laser snow cover meter*
Sunshine duration	Rotation-type sunshine duration meter*
Global solar radiation	Radiation pyranometer
Weather	Visual observation
Cloud amount/form	Visual observation
Visibility	Visual observation

* Shared with AMeDAS (the Automated Meteorological Data Acquisition System)

1.2.2 Surface Ozone Observation

The instrument used is a UV photometer from Ebara Jitsugyo Co., Ltd. (EG-2001F). In data processing, 10-minute data are calculated from 20-second sampling data, and hourly data are calculated from 10-minute data.

1.2.3 Lower-atmosphere Observation

A radiosonde attached to a tethered balloon is used to observe temperature, humidity, pressure and wind direction/speed from the ground to an altitude of approximately 1,500 m. The lower-layer wind profile from the ground to the same altitude is observed using Doppler lidar. The data collected are used to study the lower atmosphere.

1.2.4 Upper-air Observation

Upper-air observation using Vaisala RS92-SGP-type GPS radiosondes is carried out twice a day at the internationally specified times of 00 UTC (09 LST) and 12 UTC (21 LST) (Table 1.3). Observation of ozone vertical distribution using ECC-type ozonesondes is carried out at 06 UTC (15 LST) every Wednesday. Tateno was registered as a GCOS Upper-air Network (GUAN) site in March 1995. In line with GCOS recommendation, high-altitude radiosonde observation up to a pressure of 5 hPa is carried out at 12 UTC (21 LST).

Table 1.3 Upper-air observation using radiosondes at Tateno

Type	Parameter	Time	
Radiosonde	Atmospheric pressure, air temperature, humidity, wind direction/speed	0900 LST, 2100 LST*	Balloon launched 30 minutes before observation time
Ozonesonde	Ozone amount, atmospheric pressure, air temperature, wind direction/speed	1500 LST* Wednesday	

In the event of severe weather conditions such as typhoons, radiosondes are also released at 0300 LST* or 1500 LST*.

* LST (UTC + 9)

1.2.5 GPS Precipitable Water Vapor (GPS-PWV) Observation

GPS-PWV observation was started at Tateno in November 2009. The GPS receivers are the Trimble NetR8 GNSS reference type, and the antenna is the TRM559800.00 type. GPS-PWV values are derived from the GPS-PWV processing system, which includes a GPS-inferred positioning system and orbit analysis simulation (GIPSY-OASIS II) software (Webb and Zumberge, 1993).

1.2.6 Ozone Observation

Observation of the total amount and vertical distribution of ozone in the atmosphere is carried out using a Dobson ozone spectrophotometer. Analysis of observation results and improvement/development of related equipment are also implemented.

1.2.7 Ultraviolet Radiation Observation

To accurately ascertain the amount of harmful ultraviolet radiation reaching the ground, observation of global ultraviolet spectral irradiance is carried out using a Brewer spectrophotometer, and global UV-B irradiance is monitored with ultraviolet pyranometers.

1.2.8 Radiation Observation

Global solar radiation, direct solar radiation, diffuse solar radiation, reflected solar radiation, downward long-wave radiation and upward long-wave radiation are observed and studied to clarify the mechanisms behind them.

In its role as a WCRP/GCOS Baseline Surface Radiation Network (BSRN) station, Tateno has provided accurate radiation data via the BSRN data archive to researchers since 1996.

1.3 Contribution to GRUAN

Tateno was registered as a GRUAN site in September 2009, and JMA has participated from the second implementation-coordination meeting (ICM-2). At the site, inter-comparison observation of radiosondes (RS2-91 and RS92-SGP) based on double launching was carried out 120 times from December 2009 to October 2010 in conjunction with radiosonde renewal in December 2009 to gather metadata for continuity and long-range data. These inter-comparison observations were very significant work as the first case since start of GRUAN, so the results were reported by JMA at ICM-3. Tateno also provided comparison data of the two radiosondes to GRUAN's lead center in June 2011, and it is expected that the comparison observation manual will be edited based on this information and data.

Tateno began quasi-real-time report of routine upper-air observation data and radiosonde launch metadata to the GRUAN lead center by using the RSLaunchClient application since June 1, 2011. And Tateno's RsLaunchClient application was also upgraded to Ver. 0.4 on January 31, 2012.

PART 2 TEMPORAL AND SPATIAL VARIABILITY OF GPS-PWV

2.1 Introduction

JMA began to monitor the distribution of GPS-derived precipitable water vapor (GPS-PWV) over the Japanese archipelago in near-real time in May 2008. GPS-PWV values are obtained using data from the GEONET (GPS Earth Observation Network) system operated by the Geospatial Information Authority of Japan (GSI). In this system, about 1,200 GPS receivers located throughout the country at mean intervals of 15 to 25 km are used to observe crustal deformation.

The ICM-3 site report for Tateno covered examination of the spatial variability of precipitable water vapor using Japan's dense GPS network to support the discussion of co-location issues in observation. In the report, two parameters used to measure the spatial representativeness of GPS-PWV values were introduced: (1) the coefficient of spatial correlation between GPS-PWV values at Tateno and those at other stations; and (2) the standard deviation of residuals defined as differences between observational values and predicted values based on linear regression using GPS-PWV values at Tateno (the explanatory variable) and those at other stations (the dependent variable). The main results of the examination showed that a high correlation coefficient indicates a large spatial representativeness, and that an area in which the standard deviation of residuals is less than a given value can be taken as a representative area. The report also pointed out that the representative area for a specific standard deviation of residuals became larger in the cold season than in summer.

Extending on the previous examination of spatial variability, this section reports on the temporal-spatial variability of GPS-PWV. The temporal variability of precipitable water vapor can be determined from the temporal representativeness of observation values.

2.2 Methodology

To clarify the temporal-spatial variability of precipitable water vapor, GPS-PWV values at Tateno were compared with those at 75 other stations within a distance of 100 km. The values were derived from JMA's GPS-PWV processing system with GIPSY-OASIS II software. Using average 30-minute GPS-PWV values based on individual 5-minute values, the temporal-spatial variability of GPS-PWV was analyzed.

This variability is represented by the coefficient of cross-correlation (r_{ik}) between GPS-PWV values at Tateno and those at other stations (i) for the lag time (k) calculated using Equation (1).

$$r_{ik} = \frac{\sum_{j=1}^{N-k}(X_{oj} - \overline{X}_{0k})(X_{ij+k} - \overline{X}_{ik})}{\sqrt{\sum_{j=1}^{N-k}(X_{oj} - \overline{X}_{0k})^2}\sqrt{\sum_{j=1}^{N-k}(X_{ij+k} - \overline{X}_{ik})^2}} \quad (1)$$

where X_{0j} is the GPS-PWV value at Tateno at the time of observation j; X_{ij+k} is the GPS-PWV value at station i at the time of observation $j+k$ (where k denotes the lag time); $\overline{X}_{0k}$ and $\overline{X}_{ik}$ are the mean GPS-PWV values defined by $\frac{1}{N-k}\sum_{j=1}^{N-k}X_{oj}$ and $\frac{1}{N-k}\sum_{j=1}^{N-k}X_{ij+k}$, respectively; and N is the number of GPS-PWV data collected in a month. The cross-correlation coefficient for Tateno itself (r_{0k}) is the auto-correlation coefficient, and that for zero lag time (r_{i0}) is the spatial correlation coefficient.

Equation (2) gives the standard deviation of residuals (SR_{ik}) defined as differences between observational values and predicted values based on linear regression using GPS-PWV values at Tateno (the explanatory variable) and those at other stations (the dependent variable) for a specific lag time. The standard deviation of residuals is a measure of errors that cannot be explained by linear regression:

$$SR_{ik} = SD_{ik}\sqrt{1-r_{ik}^2} \quad (2)$$

where SD_{ik} denotes the standard deviation of $X_{i\,j+k}$ defined by $\sqrt{\frac{1}{N-k}\sum_{j=1}^{N-k}(X_{i\,j+k}-\overline{X}_{ik})^2}$. Since the GPS-PWV values at Tateno cannot be used to fully explain those at other stations, SR_{ik} is used as a measure of errors stemming from the temporal and spatial variability of GPS-PWV values.

2.3 Results

2.3.1 Cross-correlation Coefficient of GPS-PWV

Figure 2.1 shows the bimonthly coefficient of cross-correlation (r_{ik}) between GPS-PWV values at Tateno and those at other stations as a function of the distance from Tateno and the lag time. It can be seen that the value generally decreases with greater distance. r_{ik} for each distance decreases monotonically with greater lag times between 0 and 12 hours. While r_{ik} fell below 0.70 for lag times over 10 hours in December, April and October, relatively high values (> 0.70) were maintained in February and June. Since high cross-correlation values mean that GPS-PWV variations at Tateno can be used to explain those at other stations with lag time, a high correlation indicates spatial and temporal representativeness is large.

2.3.2 Standard Deviation of GPS-PWV Residuals

Figure 2.2 shows the bimonthly standard deviation of GPS-PWV residuals (SR_{ik}) given by Equation (2) as a function of the distance from Tateno and the lag time. It can be seen that the values generally increase with greater distance. SR_{ik} for each distance shows a monotonically increasing function of lag time between 0 and 12 hours. As shown in the figure, the values varied from month to month; for distances greater than 80 km and lag times exceeding 10 hours, SR_{ik} was relatively small (4 – 6 mm) in December and February, moderate (6 – 7 mm) in April and August, and high (7 – 10 mm) in June and October. Thus, the representative area (time) became larger (longer) in December and February than in June and October for specific SR_{ik} values.

SR_{ik} for zero distance (zero lag time) shows errors due to differences in observation times (observation points). Roughly speaking, the error for a distance of 60 km was 1 mm in February, which is equal to that for a lag time of 1.5 hours; in August, the corresponding value was 3.5 mm, which is equivalent to a lag time of 6 hours (indicated by arrows in Figure 2.2 (b) and (e)). The ratio of distance to equivalent lag time was about 40 km/hour in February and 10 km/hour in August. It can be seen that the ratio was smaller in summer than in other seasons.

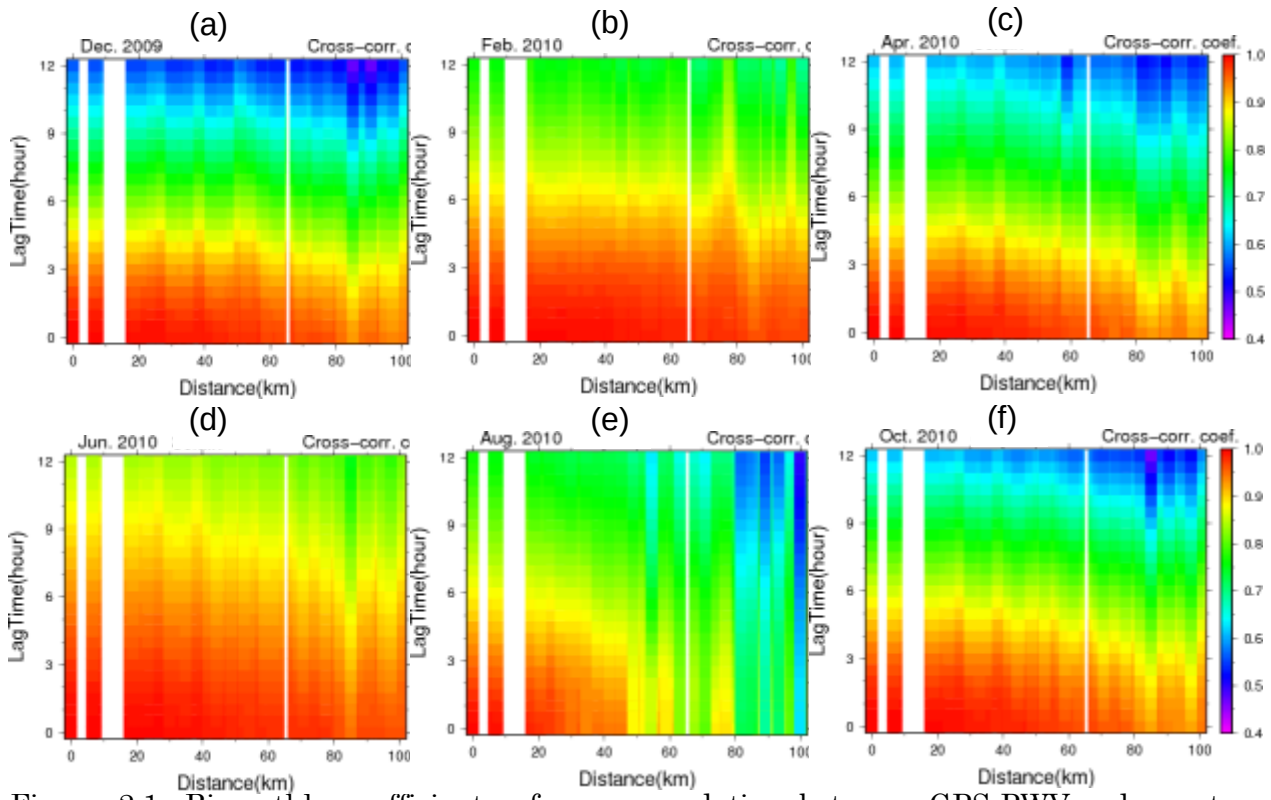

Figure 2.1. Bimonthly coefficients of cross-correlation between GPS-PWV values at Tateno and those at other stations as a function of the distance from Tateno and the lag time in (a) December 2009, (b) February 2010, (c) April 2010, (d) June 2010, (e) August 2010, and (f) October 2010

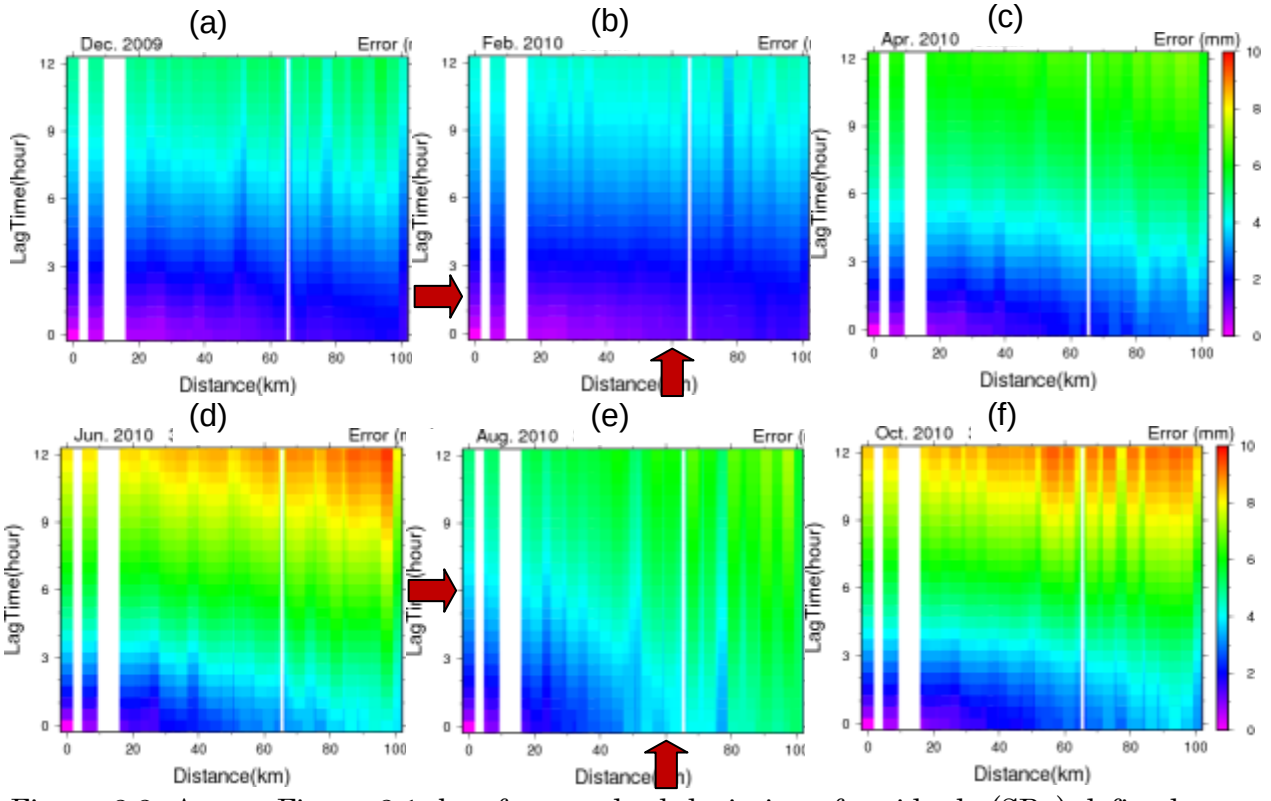

Figure 2.2. As per Figure 2.1, but for standard deviation of residuals (SR_{ik}) defined as differences between observational values and predicted values based on linear regression using GPS-PWV values at Tateno (the explanatory variable) and those at other stations (the dependent variable) for lag time. The arrows in (b) and (e) indicate a distance of 60km and a lag time where SR_{ik} values for zero distance is equivalent to a distance of 60km for zero lag time.

PART 3 STATUS OF JMA'S GLOBAL NWP SYSTEM AND EXPECTATIONS FOR UPPER-AIR DIRECT OBSERVATION

To support short- and medium-range weather forecasting, JMA operates a global NWP system encompassing a forecast model with a horizontal resolution of about 20 km and a 4D-Var data assimilation (DA) system with an inner-loop horizontal resolution of about 60 km. The DA system provides high-quality initial conditions for the forecast model using a variety of observations. Radiosonde observation is one of the most important elements of the DA system. Figure 3.1 shows the contribution rates of each observation type to the 15-hour forecast error reduction in January 2010 (WN) and August 2010 (SM). Positive values mean that the observation works to reduce the forecast error in terms of the dry energy norm. Radiosondes make the second-largest contribution after the AMSU-A microwave temperature sounders on board five polar orbiting satellites, highlighting their pivotal role in JMA's global NWP system. It was noted that the contribution rates of humidity observations are relatively small, as evaluation is performed for the dry energy norm. Dividing the contributions of radiosonde data into those from each data level shows that radiosonde values from a level above 100 hPa also contribute to a reduction of short-range forecast errors, while the levels with the largest contributions are those from 600 to 300 hPa (Figure 3.2).

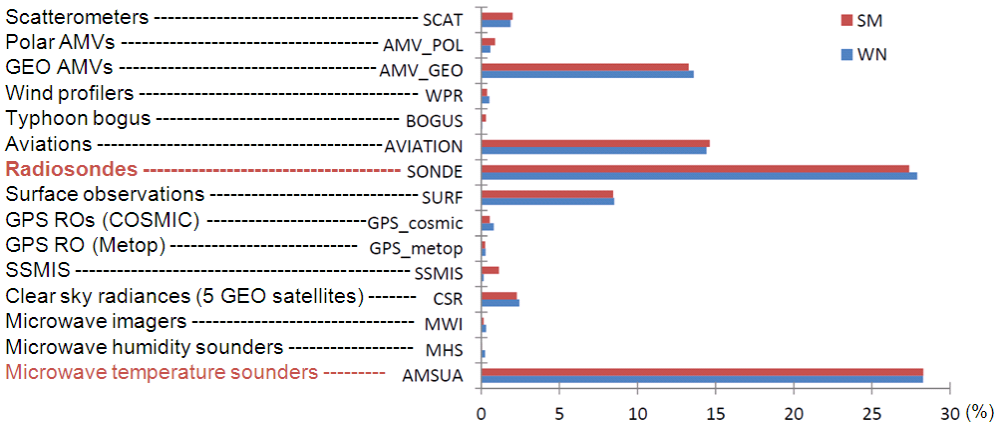

Figure 3.1. Contribution rates (%) of each observation type to 15-hour forecast error reduction in terms of dry energy norm for January 2010 (WN) and August 2010 (SM)

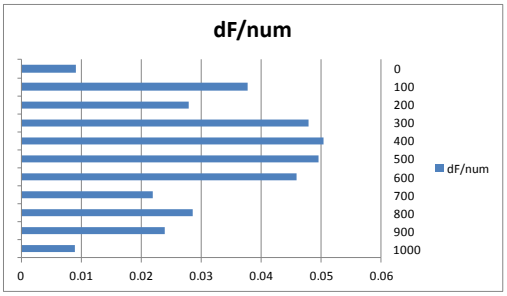

Figure 3.2. Average contribution of individual radiosonde data at every 100 hPa to 15-hour forecast error reduction in terms of dry energy norm for 00 UTC on Feb. 9, 2011. The vertical axis shows the vertical levels in hPa.

JMA plans to upgrade the global NWP system with respect to vertical-level distribution in the next high-performance computing (HPC) system, which will be become operational in 2012. Figure 3.3 shows the current and planned vertical level distributions of the global NWP system. The model top will be raised up from 0.1 hPa to 0.01 hPa, and the number of levels will be increased from 60 to 100. In the tentative plan, the number of levels around the tropopause (350 – 50 hPa) will be doubled from 13 to 27. These changes are expected to improve the ability of the system to describe sharp vertical atmospheric structures around the tropopause.

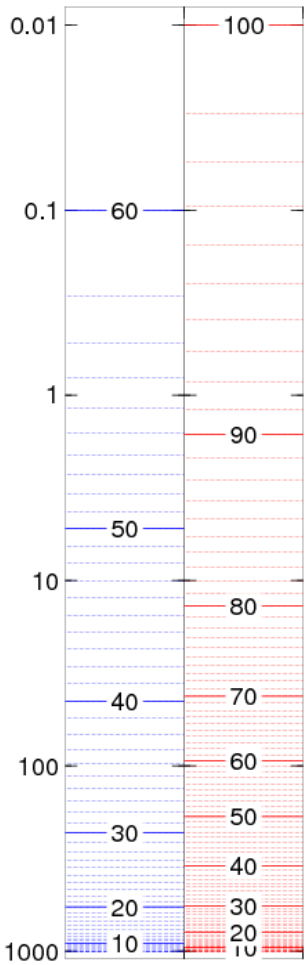

Figure 3.3. Current (left) and planned (right) vertical-level distribution of JMA's global NWP system. The vertical axis shows the vertical levels in hPa with dotted lines (for each level) and solid lines (for every 10 levels).

With the expected higher vertical resolution of the global NWP system, upper-air direct observations will become increasingly important for greater accuracy in upper-air analysis. Although microwave temperature sounders cover extensive areas (Figure 3.4 (b)), the data used are not from direct observation of temperature but from observation of radiance, which is assimilated in the NWP system with an adaptive bias correction scheme. As a result of this correction, atmospheric profiles cannot be fixed based on radiance observations alone. Since the situation is almost the same for infrared sounders (including the hyper-spectral type), other reference observations are also needed. Recently, GPS radio occultation (RO) data have emerged as being suitable for upper-air analysis, enabling bias-free global observations of refractivity or the bending angle of the atmosphere (Figure 3.4 (c)). Although their horizontal resolution is very low, the vertical resolution is very high, making the data suitable for the higher vertical resolution of the global NWP system. However, refractivity and bending angles depend on the combination of temperature and humidity. Separate observations of each component are therefore important to provide references; currently, this can be achieved only based on radiosonde observation, which is also the only type of monitoring that provides wind information at the stratospheric level. Radiosondes allow high-vertical-resolution direct observation of the atmosphere, while the horizontal distribution is insufficient and inhomogeneous. On the other hands, the both remote sensing observations (radiance and GPS-RO) show much better homogeneous horizontal distribution, while the vertical resolution of radiance observation and the horizontal resolution of GPS-RO observation

are insufficient (Table 3.1). Since all the observations are not perfect, the combinational use is important for the global observing system. And Radiosonde observation has significant role since they can serve as a reference for the remote sensing data.

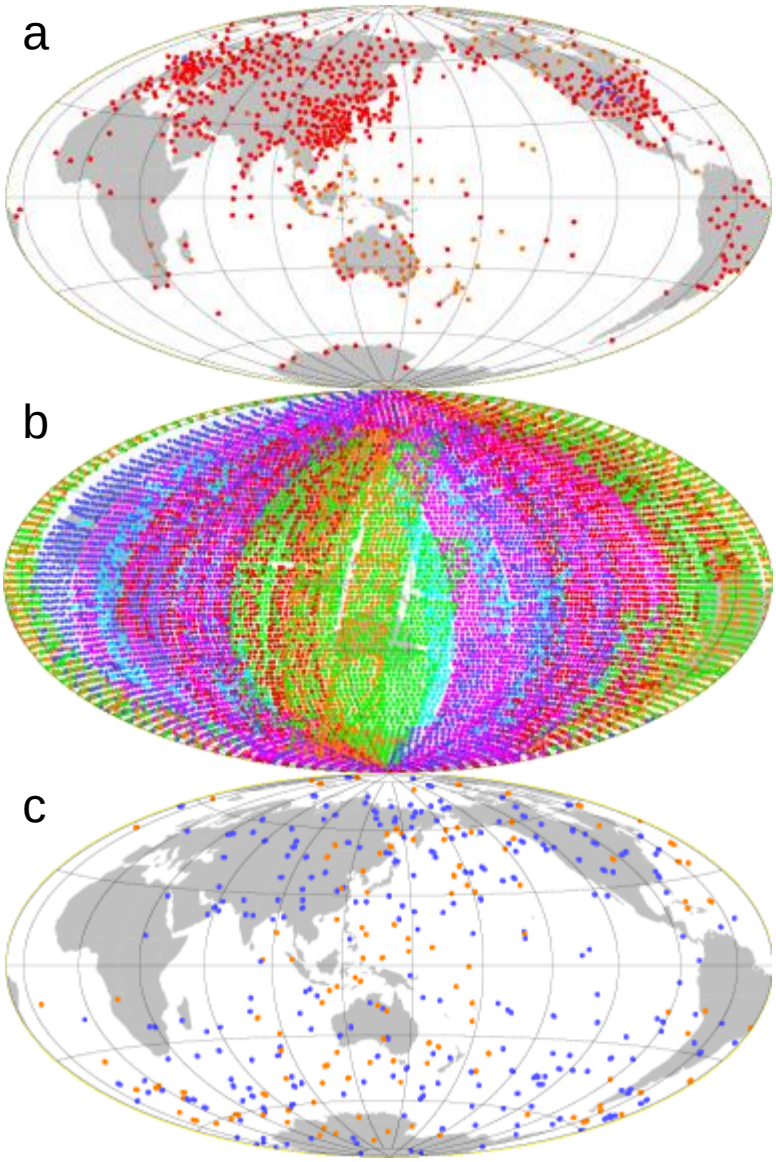

Figure 3.4. Sample distribution of assimilated observations at 12 UTC on 20 Oct., 2011. The observation time is confined to ±3 hours from the target time. Figure 3.4 (a) shows radiosonde data, 3.4 (b) shows AMSU-A microwave temperature sounder data from six polar-orbiting satellites (NOAA-15, 16, 18, 19, Aqua and Metop-A), and 3.4 (c) shows GPS-RO data from Metop-A and COSMIC.

Table 3.1. Comparison of the characteristics of each observation type

	Coverage and homogeneity	Horizontal resolution	Vertical resolution
Radiosonde	P	G	G
Radiance	G	M	P
GPS-RO	M	P	G
G: Good M: Moderate P: Poor			

4.1 Overview of JMA's Aerological Observation Network

JMA operates radiosonde observation network covering 16 stations, 8 of which are equipped with automatic balloon launcher (ABL) and hydrogen generator system (HGS). Radiosonde observation is carried out twice a day at 00 and 12 UTC, and also at 06 and 18 UTC if a typhoon is present within 300 km of the Japanese mainland. Observations are implemented on board one of two research vessels (R/V) of JMA, fitted with ASAP system, without duplicating data from fixed radiosonde sites in the western North Pacific and the seas adjacent to Japan. The GPS (Global Positioning System) wind-finding method is used for all upper-air stations and R/V as of the end of 2010. The data obtained are collected at JMA headquarters on a real-time basis.

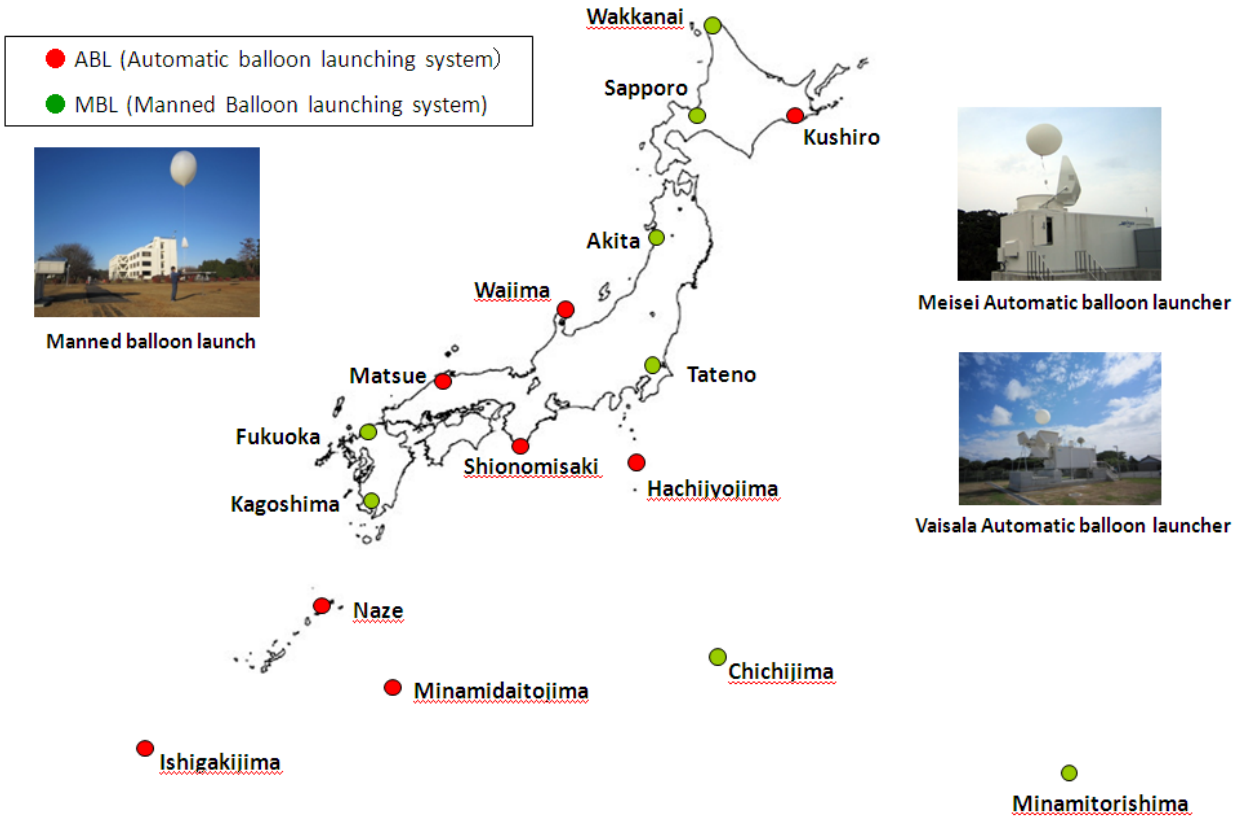

Figure 4.1 JMA's radiosonde observation network

In addition to the routine radiosonde observations performed at these 16 stations, JMA also operates wind profiler network (WINDAS) consisting of 31 wind profilers and conducts upper-air wind observations every 10 minutes up to a height of 6 – 7 km in summer and 3 – 4 km in winter. The data obtained are collected at JMA headquarters on a real-time basis. JMA plans to add two further wind profilers by March 2012.

JMA operationally calculates GPS-derived integrated water vapor using the observation data from the GPS network operated by the Geographical Survey Institute (GSI) of Japan's Ministry of Land, Infrastructure, Transport and Tourism (MLIT).

4.2 Issues of Fall Radiosondes in Urban Areas of Japan and Related Countermeasures

In Japan, radiosondes often come down in urban areas due to the densely populated nature of the country's limited land area. This often causes problems such as interruption of train services, damage to aircraft, cars, houses and other objects, and equipment becoming stuck in trees or on electric power transmission lines.

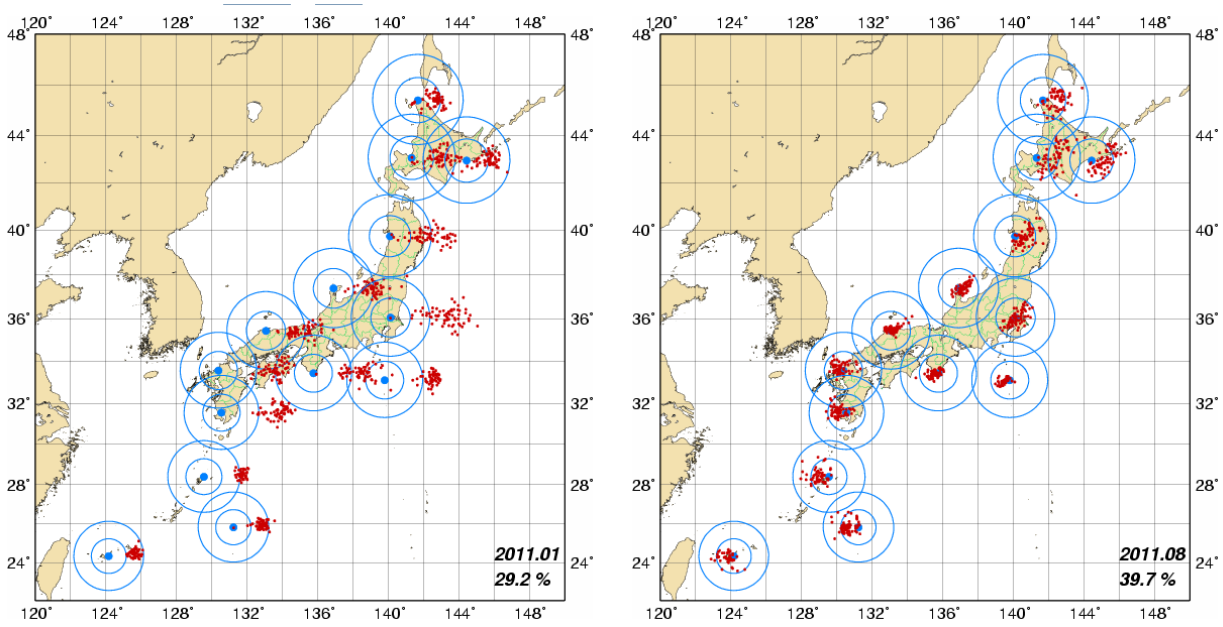

Figure 4.2 Radiosonde fall points derived from the GPS position of radiosondes for winter (January 2011; left) and summer (August 2011; right). The circles indicate distances of 100 and 200 km from each site.

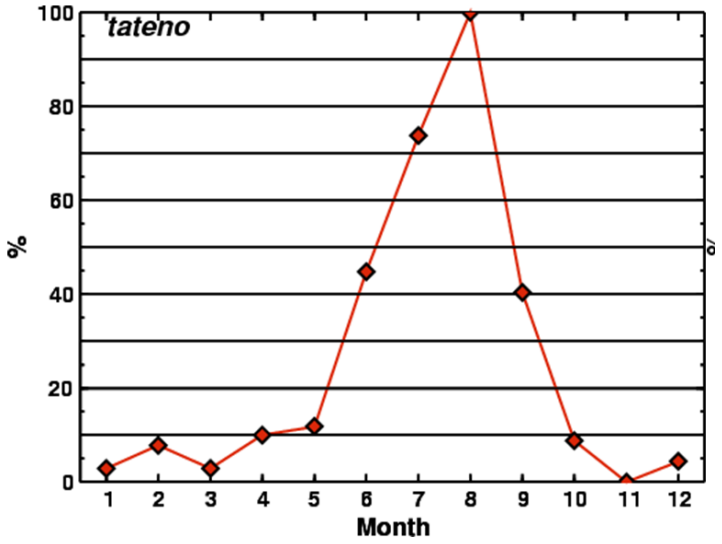

Figure 4.3 Percentages of radiosondes from Tateno falling onto land areas of Japan in 2010

JMA implements two measures to reduce the risk of accidents caused by radiosonde falls. The first is padding with dumper around radiosondes and attaching parachutes to them, and the second is shortening radiosonde strings.

With the first measure, JMA requires manufacturers to pad with dumper around radiosondes in order to reduce the chance of accidents involving units hitting objects or people. Meisei radiosondes (e.g., RS-069G RS-01G, RS2-91) have been fitted with bubble wrap as dumperpadding since 1981. JMA has also urged manufacturer Vaisala to fit padding to its units, and the company has shown a positive response in examining the possibility. As a further measure, JMA usually attaches a parachute to the radiosonde strings between the balloon and the unit.

Figure 4.4 Bubble wrap padding fitted to a radiosonde (Vaisala RS92-SGP) as per the policy adopted in July 2010

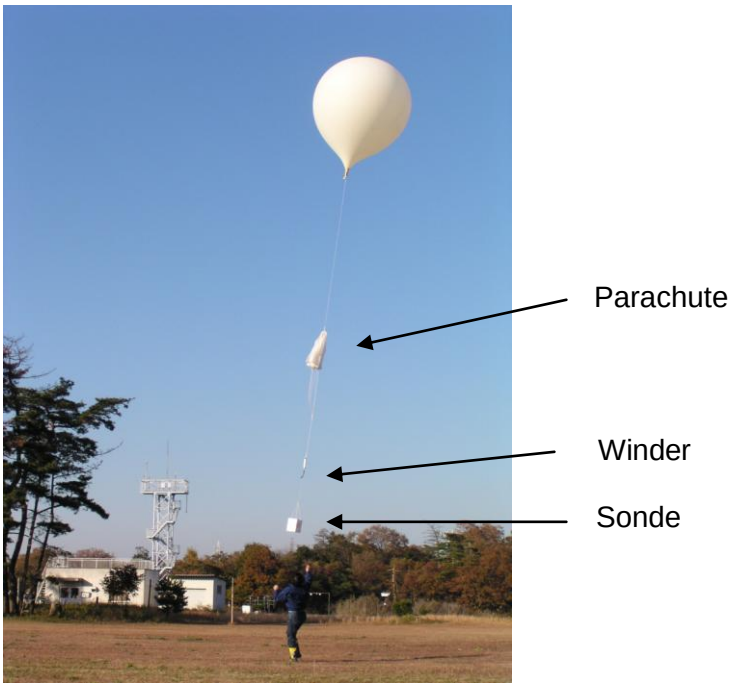

Figure 4.5 A parachute set on the strings between the balloon and the unit

With the second measure, the radiosonde strings are shortened as a trade-off for increased risk of contamination from the balloon's wake to reduce the risk of accidents involving the radiosonde catching on railroad wires and electric power lines. The normal lengths of all strings for JMA balloons are as follows:

(a) 15 m for 600 g
(b) 30 m for 1,200 g
(c) 50 m for 2,000 g

Setting a parachute on the strings automatically halves their total length during the radiosonde's descent to the ground.

To reduce the chances of radiosondes becoming caught on branches or electric power line during their ascent, JMA asks vendors of radiosonde (e.g., RS92-SGP) to make winders, which are rolled balls of string with a length of 15 m (included in the regular overall string length).

These JMA's radiosonde string specifications are based on results obtained from a long-term process of trial and error to determine optimal ways of reducing the risk of accidents.

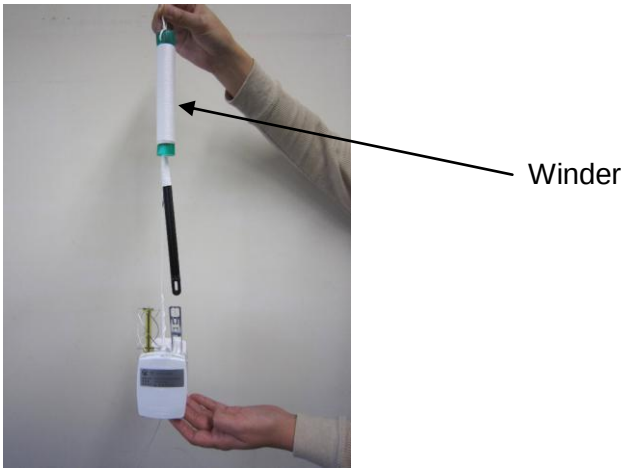

Figure 4.6 Winder

JMA has also asked manufacturers to reduce the weight of sondes, use biodegradable materials and shorten sonde strings to reduce environmental impacts and reduce the risk to public safety.

4.3 Issues of cost-effectiveness

JMA faces sufferings in maintaining its upper-air observation network due to the high operational costs involved – especially the high price of GPS radiosondes. Accordingly, manufacturers should be encouraged to be more transparent and accountable in setting sonde prices. A standardized output data format that can be used across the board for ground systems of different manufacturers also needs to be developed.

There is also an apparent need to expand the number of radiosonde stations, or at least re-activate silent stations, in data-sparse areas. Every effort should be made to avoid closing stations and to reduce the cost barrier of radiosonde operation to support sustainable operations at existing stations in such areas, where even a very small number of observations provides a significant benefit to all users.

Acknowledgements

The GEONET observation data used here were provided by the Geographical Survey Institute (GSI) of Japan. GIPSY-OASIS II software is produced by the California Institute of Technology.